

We are IntechOpen, the world's leading publisher of Open Access books Built by scientists, for scientists

6,900

Open access books available

185,000

International authors and editors

200M

Downloads

Our authors are among the

154

Countries delivered to

TOP 1%

most cited scientists

12.2%

Contributors from top 500 universities



WEB OF SCIENCE™

Selection of our books indexed in the Book Citation Index
in Web of Science™ Core Collection (BKCI)

Interested in publishing with us?
Contact book.department@intechopen.com

Numbers displayed above are based on latest data collected.
For more information visit www.intechopen.com



Calculation of the Electronic Properties and Reactivity of Nanoribbons

*Pedro Navarro-Santos, Rafael Herrera-Bucio,
Judith Aviña-Verduzco and Jose Luis Rivera*

Abstract

It has been demonstrated that matter at low dimensionality exhibits novel properties, which could be used in promising applications. An effort to understand their behavior is being through the application of computational methods providing strategies to study structures, which present greater experimental challenges. It is proven that thin and narrow carbon-based nanostructures, such as, nanoribbons show promising tunable electronic properties, particularly when they are substitutionally functionalized. This chapter is proposed as a guidance to help the readers to apply conceptual density functional theory to calculate helpful intrinsic properties, e. g., energetic, electronic and reactivity of one-dimension nanomaterial's, such as, carbon nanoribbons. As a case of study, it is discussed the effect of boron atoms on the properties of pristine carbon nanoribbons concerning the main aspect and considerations must take into account in their computational calculations.

Keywords: DFT, band structure, DOS, MEP

1. Introduction

Carbon nanoribbons (CNRs) are strips of graphene whose edges symmetry, width and cut orientation give them specific electronic properties. These carbon nanostructures have attracted the attention in both experimental and theoretical fields because of their peculiar properties, which have been studied widely in the last decade as a function of topology, width, as well as doping. [1–5] Depending the chain-type along the periodic direction, carbon nanoribbons are commonly classified either armchair carbon nanoribbons (ACNR) when these grow through dimer chains, or zigzag carbon nanoribbons (ZCNR) if those have zigzag type chains along the periodic direction. **Figure 1** shows a pristine ACNR and ZCNR respectively, their distances between their C – C edged lengths are 13.44 and 24.19 Å respectively, although there could be named referring their length and width ($M \times N$), in such case, both CNRs shown in **Figure 1** are 12x2 size.

Through different experimental techniques, it is possible to obtain carbon nanoribbons. [6–8] However, these techniques have not succeeded in controlling the edges shape of carbon nanoribbons. For example, Cai et al. [9] have proposed a chemical technique which is able to synthesize narrow nanoribbons having symmetric edges, so that, it is possible to obtain experimentally carbon nanoribbons with perfect edges

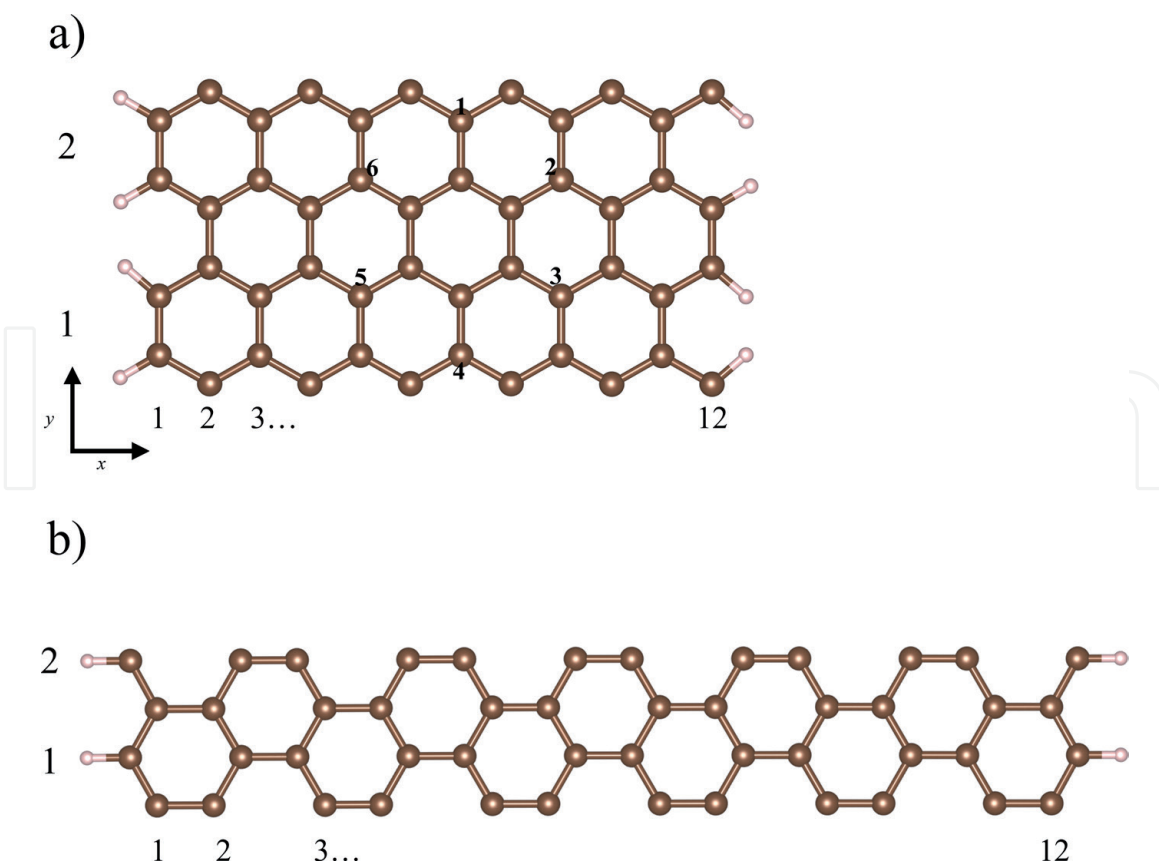


Figure 1.
Optimized structure of bare (a) ACNR and (b) ZCNR of size 12x2.

and specific topology. To date, succeeding methods to obtain CNRs come from two different strategies, namely, top-down, which refers to break down large performed carbon-base structures, i. e., CNTs and multiwall CNTs (MWCNTs) and bottom-up, i. e., using several chemical reactions to tailor building-blocks into a complex structure. **Table 1** shows a comparative chart representing synthetic strategies to obtain CNRs, employed characterization techniques, advantages and disadvantages.

Because of their finite dimension, at nanoscale, CNRs have peculiar properties associated to their electronic states close the edges, playing an important role on the reactivity. [17–22] Several theoretical models, e. g., tight binding, all electron techniques, density functional theory (DFT), etc., have been applied to explore the electronic properties, magnetic states or band structure of carbon nanoribbons. [1, 5, 23] Some of them, have focused on the zigzag topology because they intrinsically have dangling bonds at the edges. This behavior provides active sites for chemical reactions. Moreover, ZCNRs have peculiar properties, e.g., theoretical calculations have shown that ZCNRs have localized electrons largely on the edge C atoms close to the Fermi level. [4, 22] This large contribution of electronic states forms two-fold degenerate flat band at Fermi level, such that, the ground state has spin coupling of each edge ferromagnetic whereas between edges antiferromagnetic. Despite zigzag edges of synthesized carbon nanoribbons have been observed, [8] there is not direct experimental evidence about the magnetic states of ZCNRs. It was theoretically suggested that magnetism of ZCNR could be destroyed substituting defects or vacancies directly on carbon edges. [24]

On the other hand, all hydrogen-passivated ACNRs are semiconducting [22]. However, ACNRs are expected to reach the graphene limit of zero band gap for sufficiently large widths. [25]

Concerning these fascinating properties, CNRs may fit for promising technological applications, mainly if the presence of donor or acceptor impurities bring

Strategies	Method	Characteristics	Advantages	Disadvantages
Top-down	Unzipping CNTs by chemical oxidation [7]	Using potassium permanganate and sulfuric acid	The production of 100 nm wide nanoribbons	
	Etching of graphene [10]		It is possible to narrow the ribbons down to <10 nm using gas phase etching chemistry	Complicated procedures, CNRs with edges abnormalities
	Treating multiwalled CNTs [11, 12]	Longitudinal splitting of MWCNTs using hydrothermal approach	This procedure gives highly conducting CNRs with over 80% yield at low cost fabrication.	
		Intercalating lithium and ammonia into MWCNTs followed by thermal expansion	Graphene flakes attractive for many applications	Structures with large number of non-symmetric edge atoms
	Chemical Procedure Organic synthesis	Mechanical exfoliation of highly oriented pyrolyzed graphite	Produce micrometer length involving non complicated procedures	
		Chemical oxidation/ exfoliation of graphite followed by reduction of the resulting nanomaterial [13]		Resulting graphene oxide
		Cross coupling building blocks followed by dehydrogenation		Complicated procedures poorly defined edges
		Conversion of precursors inside CNTs	Because CNTs impose spatial limitations on the structure of the product, may obtain narrow CNRs	
Bottom-up	Organic synthesis [14–16]	Surface assisted polymerization followed by dehydrogenation in an ultra-high vacuum environment	Defined edge type and narrow widths, potential techniques for scale-up	Depends on the precursor's nature, which defines the ribbon's dimension

Table 1.
Comparative chart of synthetic methods to obtain nanoribbons and their advantages or disadvantages.

specific reactive properties. [26, 27] So that, this chapter is proposed as a guidance to help the readers to apply conceptual density functional theory to calculate helpful intrinsic properties, e. g., energetic, electronic and reactivity of one-dimension nanomaterial's, such as, carbon nanoribbons in order to predict or tune their properties; particularly when they are substitutional doped.

2. Structural and energetic properties

To give insights about the structural stability of nanostructures, firstly, it is suggested to evaluate if the proposal unit cell may array forming a stable crystal-line state. Usually, a structural analysis is carried out computing the cohesive energy per atoms o per unit cell. The cohesive energy (*EC*) is the energy required to disassemble a molecular system into its constituent parts. From a physical point of view, a bound (stable) system has a positive value of *EC*, which represents the energy gained during the formation of the bound state. To calculate the *EC* of ACNRs, it is necessary to obtain the optimized energy of the unit cell being aware of the well converged energy with respect to the *k*-points and the cutoff energy for the planewave basis set, evaluating the impact of the exchange-correlation functional used and its ability to accurately describe both the atom and bulk phase.

Although *EC* is a reference to know the stability of bulk materials, it differs from a nanoparticle. [28–30] At nanoscale, size effects on the cohesive energy of nanoparticles has been demonstrated, which decreases with decreasing the particle size. [31] However, slight differences of *EC* are found when nuclei radii of constituent are similar, which do difficult to analyze or find a trend, e. g., the effect of the relative position of dopants along the NRs. For example, **Table 2** shows the calculated values of *EC* of armchair carbon nanoribbons (ACNR) doped with boron atoms in randomly (ACNR-R) and forming one B nanoisland (ACNR-I) arrangements compared with those pristine ACNRS of size 16x2, 20x2, 16x2 and 20x4 respectively. [32] The arrangement of the nanoisland (ACNR-I) explained in this section is shown in part (a) of **Figure 1** numbering from 1 to 6 the C atoms are substituted for impurities. Note that, B doping slightly reduces the cohesive energy of ACNRs compared with the pristine ones with similar *EC* values mainly found in the largest B-ACNRs. However, at lower doping concentrations, i. e. in the case of the largest ACNR (20x4) very close values of *EC* are obtained which makes difficult to observe a trend.

Because of these CNRs has 3 different chemical species, *EC* does not provide a suitable way to evaluate the relative stability. **Table 2** also shows in brackets the calculated values of the Gibbs free formation energy to take into account the chemical composition of ACNRs. The relative thermodynamic stability that is considered to evaluate the relative stability of multicomponent systems. This approach has been used in binary and tertiary phase thermodynamics and nanostructures other than NRs. [25, 33, 34] it can be calculated by using the following expression:

$$\delta G = E(x) + \sum_{i=1}^n x_i \mu_i \tag{1}$$

MxN	Pristine	ACNR-R	ACNR-I
16x2	7.224 (0.003)	6.992 (−0.272)	7.003 (−0.291)
20x2	7.338 (0.002)	7.143 (−0.224)	7.158 (−0.239)
16x4	7.225 (0.003)	7.112 (−0.142)	7.116 (−0.147)
20x4	7.338 (0.002)	7.249 (−0.119)	7.250 (−0.130)

Table 2.
Cohesive per atom (Gibbs free) energy in eV of pristine and B-doped ACNRs of randomly (ANCR-R) and forming a B-nanoisland (ACNR-I) [32].

where $E(x)$ is the binding energy per atom of the B-ACNR for the example shown in **Table 1**, x_i corresponds to the molar fraction of the conformant components (H, N, B, C) which satisfies $\sum x_i = 1$, where $x_i = \frac{n_i}{n_T}$, being n_i the number of atoms of specie i in the unit cell and n_T the total number of atoms conforming the unit cell. The chemical potential (μ_i) can be approximate as the binding energy per atom of the singlet ground state of the H_2 , the triplet ground state of the B_2 molecule and the cohesive energy per atom of the graphene sheet respectively. Note that positive values of δG represent a metastable structure with respect to the conforming constituents, whereas negative values of δG refer to stable structures in accordance with their constituents. As we can observe in **Table 2**, δG suggests that the arrangement of B-nanoisland leads to stabilize energetically the pristine carbon nanoribbons more than the randomly cases.

3. Electronic properties of nanoribbons

The electronic properties of nanoribbons can be inferred from the band structure and total and local density of states (DOS and LDOS) respectively. For the case of NRs, these calculations are relatively simple because they are computed sampling the Brillouin zone only in one direction, i. e., the grown direction from 0 to gamma point. We recommend to use a denser grid than the case of the total energy calculations, including a Gaussian smearing (of width 0.01 eV) to improve the convergence of the integrals of the energy levels for the band structure calculations, for DOS calculations, to use the tetrahedron method with Blöchl corrections. [35, 36]

Pristine CNRs with hydrogen passivated armchair edges passivated are direct bandgap semiconducting, which decreases as their width increases. The edges of ACNRs play an important role on their electronic properties and reactivity because of quantum confinement gaps, which can be characterized by $\Delta_{Na} \sim \omega_a^{-1}$. [19, 23, 37]

In order to evaluate the electronic nature of nanoribbons, firstly, spin-polarized and non-spin polarized solutions of the Kohn-Sham equations must be taken into account to evaluate possible magnetic configurations, as found in zigzag carbon nanoribbons, [38] that implies the magnetic state is the most stable. For armchair ribbons, the non-magnetic state is always the most stable [22] even for ACNRs doped with boron atoms, [32] so that, for simplicity, we consider the armchair topology as a case of study.

The electronic behavior of ACNRs can be tuned for the influence of substitutional dopants. To illustrate this fact, we think about a unit cell containing one pristine CNR with even number of electrons of valence. If we replace only one carbon atom (with 4 valence electrons) for B (3 valence electrons) or N (5 valence electrons) such change gives one unit cell with odd number of valence electrons, in such cases is necessary to search for spin polarized solutions of the Kohn Sham equation, i. e, to evaluate if there are significant differences with respect to the non-spin polarized solution.

Figure 2 presents the band structure, total density of states and local density of states of dopants (shown in line red) of the 12x2 ACNR pristine, B-doped and N-doped substituting two dopants on positions 3 and 4 using the numbering shown in **Figure 1**. Note that, the pristine ACNR is a semiconducting in agreement with the literature [22] and the positive doping caused for the B moves the Fermi level (EF) to lower energies meanwhile the negative doping related with the N moves the EF

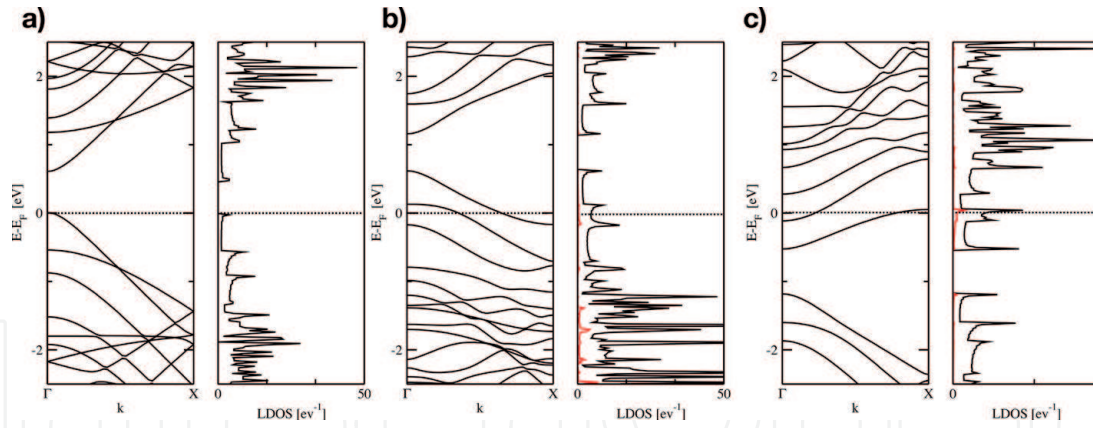


Figure 2. Band structure and DOS of (a) pristine, (b) B-doped and (c) N-doped ACNRs of size 12x2.

to higher energies with respect to the pristine one. In both cases, the closest energy bands to EF are partially unoccupied and occupied respectively giving rise to metallic behavior in both cases.

4. Reactivity of nanoribbons

In order to explore the reactivity of 1D nanomaterials, such as nanoribbons, it is mandatory to use appropriate reactivity descriptor. However, there is not a well established criteria to accomplish this task without prior knowing of an adsorption mechanism or experimental evidence, particularly for doped nanoribbons.

This is why, it is suggested the employment of two reactivity descriptors that are able to cover covalent and non-covalent interactions. The first one is the electrostatic potential, defined as:

$$V(\mathbf{r}) = \sum_A \frac{Z_A}{|\mathbf{R}_A - \mathbf{r}|} - \int \frac{\rho(\mathbf{r}') d\mathbf{r}'}{|\mathbf{r}' - \mathbf{r}|} \quad (2)$$

Where Z_A and R_A are the atomic number of nucleus A and its position respectively, $|\mathbf{R}_A - \mathbf{r}|$ is its distance from the point \mathbf{r} and $\rho(\mathbf{r}')$ is the electron density in each volume element. This descriptor provides the response of electron density when a positive unit charge is approaching, which is commonly plotted in a color scheme. Because of the electrostatic potential $V(\mathbf{r})$, is a local property, it has one value for each \mathbf{r} point in the space surrounding a molecule or unit cell, so that, depending the nature of the ions (for instance positive or negative nature), the electrostatic potential will depend on the radial distance \mathbf{r} from the nucleus.

Commonly is followed that the contour of the electrostatic potential is plotted on the isovalue of the molecular electron density, for example, see the Bader's suggestion. [39] Be aware that, the chosen outer electron density contour depends on the Van der Waals radii of involving ions, which should reflect the molecular properties we want to observe, e. g., lone pairs, strained bonds, conjugated π systems, etc.

To illustrate, **Figure 3** shows the electrostatic potential of pristine, B-doped and N-doped carbon nanoribbons of size 12x2 plotted on the electron density surface of value 0.001 au, computed by using the generalized gradient approximation (GGA) in the form proposed by Perdew et al. for exchange-correlation

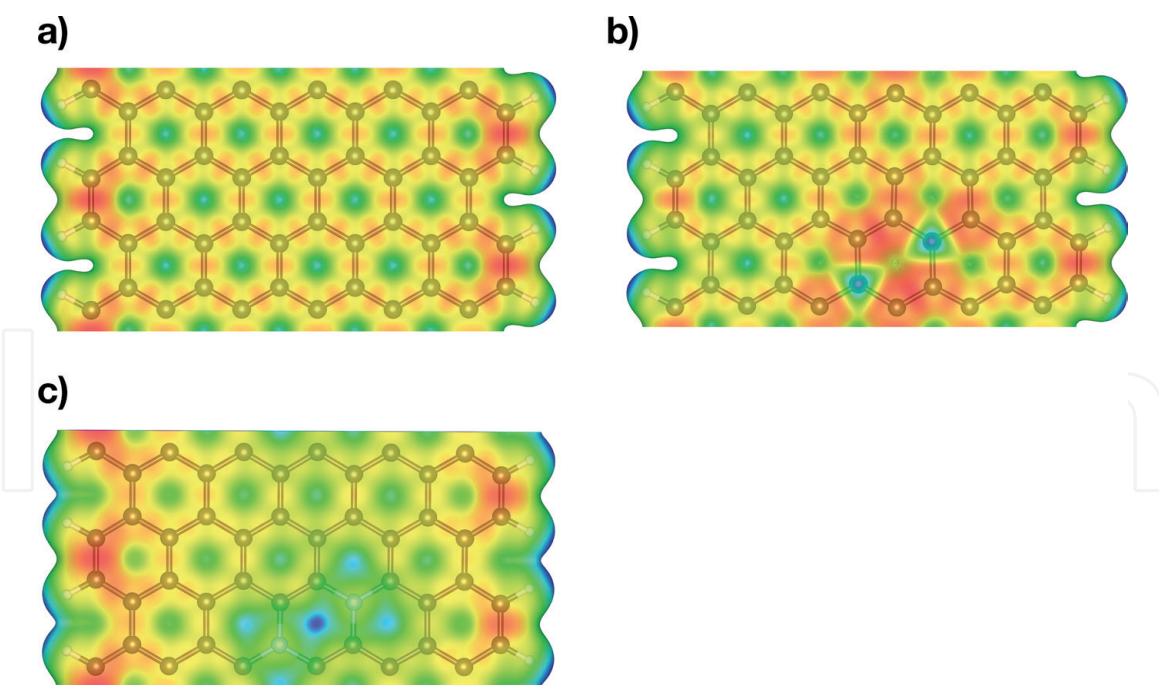


Figure 3.
 Molecular electrostatic potential of the nanoribbons (a) pristine (b) B-doped and (c) N-doped of size 12x2.

functional. **Figure 3** was built in the software VESTA [40] plotting the charge file and then, adding the cube file containing the local potential. The color scheme used in **Figure 3** represents in blue, regions where a positive charge may repel each other, unlike in red, it represents regions where a positive charge, ion or chemical group can interact.

We can observe from **Figure 3a** that, hydrogens are weak positive meanwhile the delocalized charge is distributed along the carbon atoms, particularly found in the edged carbons, which is in agreement with the DOS of pristine ACNRs. The lacking of π electrons of the boron atoms is particularly observed in **Figure 3b**, which influences over their neighbor carbon atoms finding localized charge in such region. On the other hand, the N doping influences over the edges with more negative electrostatic potential than the pristine carbon nanoribbon.

The second reactivity descriptor is the Fukui or frontier functions (Ffs), helpful chemical reactivity descriptors for process controlled by electron transfer. Ffs were introduced for the first time by Parr and Yang, [41], which is convinced from the area of research so-called conceptual Density Functional Theory given by Geerlings in a comprehensive way. [42] Fukui functions play an important role linking the Molecular Orbital Theory with the HSAB principle, [43] they are defined as the change of the electronic density with respect to number of electrons (N), considering the nuclei position fixed, i.e. constant external potential $v(r)$:

$$f(r) = \left(\frac{\partial \rho(r)}{\partial N} \right)_{v(r)} \quad (3)$$

Due to the discontinuity of the above equation with respect to N , in a finite difference approximation three functions can be defined as:

$$f_{v,N}^+(r) = \rho_{v,N+1}(r) - \rho_{v,N}(r) \quad (4)$$

$$f_{v,N}^{-}(r) = \rho_{v,N}(r) - \rho_{v,N-1}(r) \quad (5)$$

$$f_{v,N}^0(r) = 0.5(\rho_{v,N+1}(r) - \rho_{v,N-1}(r)) \quad (6)$$

Where $\rho_{v,N+1}(r)$, $\rho_{v,N}(r)$, and $\rho_{v,N-1}(r)$, are the electronic densities of the system with $N + 1$, N , and $N-1$ electrons, respectively, all with the ground state geometry of the N electron system. Expressions 4–6 concern the Fukui function for: nucleophilic attack, the chemical change where a molecule gains an electron; electrophilic attack, when a molecule loses charge; and for free radical attacks. [44]

Although, the finite difference approximation to the Fukui functions works for a specific set of configurations whilst for others is worthless to implement (i.e., full configuration interaction), [45] in most cases they are considered a reliable descriptor to indicate how the electron (incoming or outgoing) is redistributed in regions of the molecules. [46] Chemical reactivity is based on the assumption that, when molecules A and B interact in order to form a product AB, occurs a molecular densities-perturbation. [47] As the electronic density contains all sort of information, the chemical reactivity has to be reflected within its sensitivity to infinitesimal electron changes at constant external potential $v(r)$. Calculation of the frontier orbitals (HOMO or LUMO) are unambiguously defined. Within the frozen orbital approximation, [48] Ffs can be written in terms of the Kohn-Sham orbitals as follows:

$$f^{+}(r) = |\phi_{v,N}^{LUMO}(r)|^2 + \sum_{i=1}^N \left(\frac{\partial |\phi_i(r)|}{\partial N} \right) \approx \rho_{v,N}^{LUMO}(r) \quad (7)$$

$$f^{-}(r) = |\phi_{v,N}^{HOMO}(r)|^2 + \sum_{i=1}^N \left(\frac{\partial |\phi_i(r)|}{\partial N} \right) \approx \rho_{v,N}^{HOMO}(r) \quad (8)$$

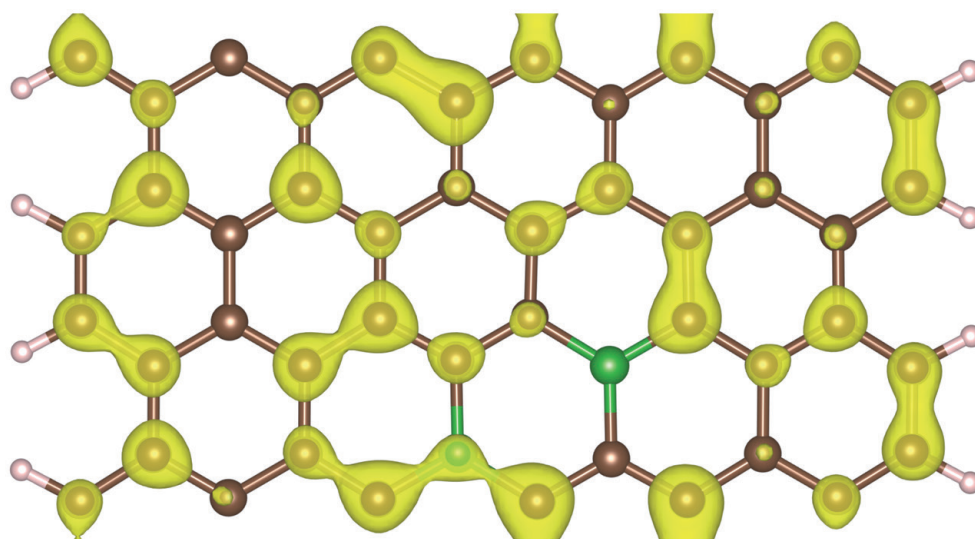
In molecules, the relaxation term is usually very small for the discrete nature of Kohn Sham orbitals. So that, if Eqs. 7 and 8 neglect the second-order variations in the electron density, Ffs may approximate to the electron densities of its frontier orbitals.

On the other hand, referring to periodic systems, it is difficult to identify one frontier state because of the continuous character of the Blöch states, which makes difficult to compute the Fukui functions in DFT of the solid state. Although there is scarcely literature on this topic, a very useful reference for the numerical calculation of the condensed Ffs in periodic boundary conditions within the DFT applied to oxide bulk and surfaces is found here. [49]

One qualitative way to obtain Ffs for delocalized periodic systems, such as, the carbon nanoribbons is to extract its electron density and evaluate it by using the Eq. (7) and (8) respectively. From the electronic structure of these nanomaterials we can observe that only one occupied electronic band contributes below and above the Fermi level.

Figure 3 depicts the Ffs evaluated for electrophilic attacks respectively for B-doped and N-doped armchair carbon nanoribbons of size 12x2 with doping made on positions 3 and 4 using the numbering shown in **Figure 1**.

a)



b)

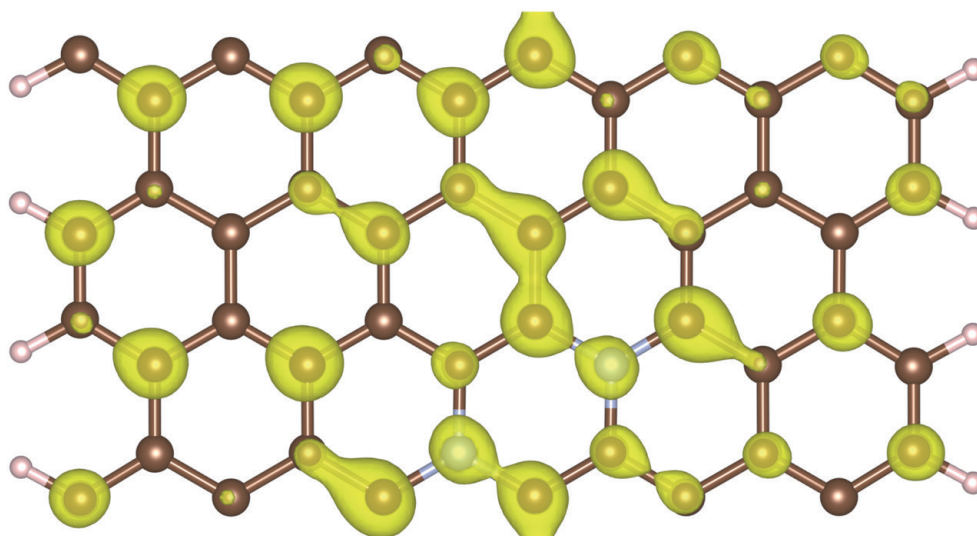


Figure 4.
 Fukui functions for nucleophilic attack of (a) B-doped and (b) N-doped ACNRs of size 12x2.

We observe from **Figure 4** that the B atoms contributes to form regions where an electrophilic attack can occur on the doped nanoribbons, i. e. larges values of f^- mean regions where the ACNR will lose charge to stabilize it in a chemical change.

The electrostatic potential and the Fukui functions provide information on the local selectivity for donor-acceptor interactions. In here, the electrostatic potential describes the long-range non-covalent interactions. [50] The evaluation of the incoming charge distribution on nanoribbons states that “The Fukui function is strong while regions of a molecule are chemically softer than the regions where the Fukui function is weak. By invoking the hard and soft acid and bases (HSAB) principle [51] in a local sense, it is possible to establish the behavior of the different sites as function of hard or soft reagents (adsorbates)”. [32, 52–54] **Figure 4** shows the Fukui functions for electrophilic attack, calculated by using Eq. (8), we observe the contribution of doping particularly on the neighboring carbon atoms. Indeed, from parts (b) and (c) of **Figure 2** is observed the electronic states of dopants contributing near the Fermi level.

5. Conclusions

In this chapter is presented how the energetic, electronic and reactivity of can be calculated for 1D nanomaterial's, such as, carbon nanoribbons. Although the carbon nanoribbons are used as case of study, this methodology can be applied for other kind of chemical compositions, in our experience we have explore the reactivity and stability of doped boron nitride at nanoscale. It is worthy to mention that, the evaluation of Fukui functions in periodic boundary conditions is limited in the usual computational approaches, so that, we suggest to support and compare such analysis with others e. g., charge analysis, global reactivity descriptors depending the nature of the involving chemical species.

Acknowledgements

PNS thanks to CONACYT for grant number 252239 and Cátedras CONACYT for Research Fellow.

Conflict of interest

The authors declare no conflict of interest.

Author details

Pedro Navarro-Santos^{1*}, Rafael Herrera-Bucio², Judit Aviña-Verduzco² and Jose Luis Rivera³


¹ CONACYT-Universidad Michoacana de San Nicolás de Hidalgo, Edif. B-1, Francisco J. Múgica, s/n, Morelia 58030, Michoacán, Mexico

² Instituto de Investigaciones Químico-Biológicas, Universidad Michoacana de San Nicolás de Hidalgo, Edif. B-1, Francisco J. Múgica, s/n, Morelia 58030, Michoacán, Mexico

³ Facultad de Ciencias Fisico-Matemáticas, Universidad Michoacana de San Nicolás de Hidalgo, Francisco J. Múgica, s/n, Morelia 58030, Michoacán, Mexico

*Address all correspondence to: pnavarro@conacyt.mx

IntechOpen

© 2020 The Author(s). Licensee IntechOpen. This chapter is distributed under the terms of the Creative Commons Attribution License (<http://creativecommons.org/licenses/by/3.0>), which permits unrestricted use, distribution, and reproduction in any medium, provided the original work is properly cited. 

References

- [1] Nakada K, Fujita M, Dresselhaus G, Dresselhaus MS. Edge state in graphene ribbons: Nanometer size effect and edge shape dependence. *Phys Rev B*. 1996;**54**(24):17954-17961
- [2] Martins TB, Miwa RH, da Silva AJR, Fazzio A. Electronic and Transport Properties of Boron-Doped Graphene Nanoribbons. *Phys Rev Lett*. 2007;**98**(19):196803.
- [3] Jiang D-e, Sumpter BG, Dai S. Unique chemical reactivity of a graphene nanoribbon's zigzag edge. *J Chem Phys*. 2007;**126**(13):-.
- [4] Yu SS, Zheng WT, Wen QB, Jiang Q. First principle calculations of the electronic properties of nitrogen-doped carbon nanoribbons with zigzag edges. *Carbon*. 2008;**46**(3):537-43.
- [5] Dutta S, Manna AK, Pati SK. Intrinsic Half-Metallicity in Modified Graphene Nanoribbons. *Phys Rev Lett*. 2009;**102**(9):096601.
- [6] Berger C, Song Z, Li X, Wu X, Brown N, Naud C, et al. Electronic Confinement and Coherence in Patterned Epitaxial Graphene. *Science*. 2006;**312**(5777):1191-6.
- [7] Kosynkin DV, Higginbotham AL, Sinitskii A, Lomeda JR, Dimiev A, Price BK, et al. Longitudinal unzipping of carbon nanotubes to form graphene nanoribbons. *Nature*. 2009;**458**(7240):872-6.
- [8] Tapasztó L, Dobrik G, Lambin P, Biró LP. Tailoring the atomic structure of graphene nanoribbons by scanning tunnelling microscope lithography. *Nature Nanotechnology*. 2008;**3**(7):397-401.
- [9] Cai J, Ruffieux P, Jaafar R, Bieri M, Braun T, Blankenburg S, et al. Atomically precise bottom-up fabrication of graphene nanoribbons. *Nature*. 2010;**466**(7305):470-3.
- [10] Wang X, Dai H. Etching and narrowing of graphene from the edges. *Nature Chemistry*. 2010;**2**(8):661-5.
- [11] Cano-Márquez AG, Rodríguez-Macías FJ, Campos-Delgado J, Espinosa-González CG, Tristán-López F, Ramírez-González D, et al. Ex-MWNTs: Graphene Sheets and Ribbons Produced by Lithium Intercalation and Exfoliation of Carbon Nanotubes. *Nano Lett*. 2009;**9**(4):1527-33.
- [12] Shinde DB, Majumder M, Pillai VK. Counter-ion Dependent, Longitudinal Unzipping of Multi-Walled Carbon Nanotubes to Highly Conductive and Transparent Graphene Nanoribbons. *Scientific Reports*. 2014;**4**(1):4363.
- [13] Stankovich S, Dikin DA, Dommett GHB, Kohlhaas KM, Zimney EJ, Stach EA, et al. Graphene-based composite materials. *Nature*. 2006;**442**(7100):282-6.
- [14] Vo TH, Shekhirev M, Kunkel DA, Orange F, Guinel MJF, Enders A, et al. Bottom-up solution synthesis of narrow nitrogen-doped graphene nanoribbons. *Chem Commun*. 2014;**50**(32):4172-4.
- [15] Sakaguchi H, Kawagoe Y, Hirano Y, Iruka T, Yano M, Nakae T. Width-Controlled Sub-Nanometer Graphene Nanoribbon Films Synthesized by Radical-Polymerized Chemical Vapor Deposition. 2014;**26**(24):4134-8.
- [16] Yang X, Dou X, Rouhanipour A, Zhi L, Räder HJ, Müllen K. Two-Dimensional Graphene Nanoribbons. *J Am Chem Soc*. 2008;**130**(13):4216-7.
- [17] Cervantes-Sodi F, Csányi G, Piscanec S, Ferrari AC. Edge-functionalized and substitutionally

doped graphene nanoribbons:
Electronic and spin properties. Phys
Rev B. 2008;77(16):165427.

[18] Ezawa M. Peculiar width
dependence of the electronic properties
of carbon nanoribbons. Phys Rev B.
2006;73(4):045432.

[19] Fujita M, Wakabayashi K, Nakada K,
Kusakabe K. Peculiar Localized State at
Zigzag Graphite Edge. J Phys Soc Jpn.
1996;65(7):1920-3.

[20] Lee Y-L, Lee Y-W. Ground state of
graphite ribbons with zigzag edges. Phys
Rev B. 2002;66(24):245402.

[21] Miyamoto Y, Nakada K, Fujita M.
First-principles study of edge states of
H-terminated graphitic ribbons. Phys
Rev B. 1999;60(23):16211-.

[22] Son Y-W, Cohen ML, Louie SG.
Energy Gaps in Graphene Nanoribbons.
Phys Rev Lett. 2006;97(21):216803.

[23] Wakabayashi K, Fujita M, Ajiki H,
Sigrist M. Electronic and magnetic
properties of nanographite ribbons.
Phys Rev B. 1999;59(12):8271-82.

[24] Huang B, Liu F, Wu J, Gu
B-L, Duan W. Suppression of spin
polarization in graphene nanoribbons
by edge defects and impurities. Phys
Rev B. 2008;77(15):153411.

[25] Barone V, Hod O, Scuseria GE.
Electronic Structure and Stability
of Semiconducting Graphene
Nanoribbons. Nano Lett.
2006;6(12):2748-54.

[26] Novoselov KS, Geim AK,
Morozov SV, Jiang D, Zhang Y,
Dubonos SV, et al. Electric Field Effect
in Atomically Thin Carbon Films.
Science. 2004;306(5696):666-9.

[27] Zhang Y, Tan Y-W, Stormer HL,
Kim P. Experimental observation
of the quantum Hall effect and

Berry's phase in graphene. Nature.
2005;438(7065):201-4.

[28] Jiang Q, Aya N, Shi FG. Nanotube
size-dependent melting of single
crystals in carbon nanotubes. Appl
Phys A. 1997;64(6):627-9.

[29] David TB, Lereah Y, Deutscher G,
Kofman R, Cheyssac P. Solid-liquid
transition in ultra-fine lead particles.
Philos Mag A. 1995;71(5):1135-43.

[30] Lamber R, Wetjen S, Jaeger NI. Size
dependence of the lattice parameter of
small palladium particles. Phys Rev B.
1995;51(16):10968-71.

[31] Qi WH, Wang MP. Size effect on the
cohesive energy of nanoparticle. J Mater
Sci Lett. 2002;21(22):1743-5.

[32] Navarro-Santos P,
Ricardo-Chávez JL, Reyes-Reyes M,
Rivera JL, López-Sandoval R. Tuning
the electronic properties of armchair
carbon nanoribbons by a selective
boron doping. J Phys: Condens Matter.
2010;22(50):505302.

[33] Dumitrică T, Hua M,
Yakobson BI. Endohedral silicon
nanotubes as thinnest silicide wires.
Phys Rev B. 2004;70(24):241303.

[34] Kan E-j, Li Z, Yang J, Hou JG. Half-
Metallicity in Edge-Modified Zigzag
Graphene Nanoribbons. J Am Chem
Soc. 2008;130(13):4224-5.

[35] Kresse G, Joubert D. From ultrasoft
pseudopotentials to the projector
augmented-wave method. Phys Rev B.
1999;59(3):1758-75.

[36] Blöchl PE. Projector augmented-
wave method. Phys Rev B.
1994;50(24):17953-79.

[37] Abanin DA, Lee PA, Levitov LS.
Spin-Filtered Edge States and Quantum
Hall Effect in Graphene. Phys Rev Lett.
2006;96(17):176803.

- [38] Magda GZ, Jin X, Hagymási I, Vancsó P, Osváth Z, Nemes-Incze P, et al. Room-temperature magnetic order on zigzag edges of narrow graphene nanoribbons. *Nature*. 2014;514(7524):608-11.
- [39] Bader RFW, Carroll MT, Cheeseman JR, Chang C. Properties of atoms in molecules: atomic volumes. *J Am Chem Soc*. 1987;109(26):7968-79.
- [40] Momma K, Izumi F. VESTA 3 for three-dimensional visualization of crystal, volumetric and morphology data. *J Appl Crystallogr*. 2011;44(6):1272-6.
- [41] Yang W, Parr RG. Hardness, softness, and the fukui function in the electronic theory of metals and catalysis. 1985;82(20):6723-6.
- [42] Geerlings P, De Proft F, Langenaeker W. Conceptual Density Functional Theory. *Chem Rev*. 2003;103(5):1793-874.
- [43] Li Y, Evans JNS. The Fukui Function: A Key Concept Linking Frontier Molecular Orbital Theory and the Hard-Soft-Acid-Base Principle. *J Am Chem Soc*. 1995;117(29):7756-9.
- [44] Yang W, Mortier WJ. The use of global and local molecular parameters for the analysis of the gas-phase basicity of amines. *J Am Chem Soc*. 1986;108(19):5708-11.
- [45] Ayers PW, De Proft F, Borgoo A, Geerlings P. Computing Fukui functions without differentiating with respect to electron number. I. Fundamentals. *J Chem Phys*. 2007;126(22):224107.
- [46] Chermette H, Boulet P, Stefan P. *Reviews of Modern Quantum Chemistry: A Celebration of the Contributions of Robert G. Parr* Parr. Singapore: World Scientific; 2002.
- [47] L. GJ. *Structure and Bonding*. Berlin: Springer-Verlag; 1993. 268 p.
- [48] Ayers PW, Yang W, Bartolotti LJ. *Chemical Reactivity Theory: A Density Functional View*: CRC Press; 2009. 610 p.
- [49] Cerón ML, Gomez T, Calatayud M, Cárdenas C. Computing the Fukui Function in Solid-State Chemistry: Application to Alkaline Earth Oxides Bulk and Surfaces. *The Journal of Physical Chemistry A*. 2020;124(14):2826-33.
- [50] Politzer P, Murray JS, Peralta-Inga Z. Molecular surface electrostatic potentials in relation to noncovalent interactions in biological systems. *Int J Quantum Chem*. 2001;85(6):676-84.
- [51] Pearson RG. Hard and Soft Acids and Bases. *J Am Chem Soc*. 1963;85(22):3533-9.
- [52] Morales-Palacios FG, Navarro-Santos P, Beiza-Granados L, Rivera JL, García-Gutiérrez HA, Herrera-Bucio R. Conjugate addition between syringol and a captodative olefin catalyzed by BF₃. 2019;32(12):e4011.
- [53] Rivera JL, Navarro-Santos P, Guerra-Gonzalez R, Lima E. Interaction of Refractory Dibenzothiophenes and Polymerizable Structures. *International Journal of Polymer Science*. 2014;2014:11.
- [54] Rivera JL, Navarro-Santos P, Hernandez-Gonzalez L, Guerra-Gonzalez R. Reactivity of Alkyldibenzothiophenes Using Theoretical Descriptors. *J Chem*. 2014;2014:8.